Suppression of nonradiative recombination process in directly Si-doped InAs/GaAs quantum dots

Kita, Takashi

Hasagawa, Ryuichi

Inoue, Tomoya

(Citation)
Journal of Applied Physics,110(10):103511-103511

(Issue Date)
2011-11-15

(Resource Type)
journal article

(Version)
Version of Record

(URL)
https://hdl.handle.net/20.500.14094/90001630

Suppression of nonradiative recombination process in directly Si-doped InAs/GaAs quantum dots

Takashi Kita,[a] Ryuichi Hasagawa, and Tomoya Inoue
Department of Electrical and Electronic Engineering, Faculty of Engineering, Kobe University, Rokkodai 1-1, Nada, Kobe 657-8501, Japan

(Received 22 July 2011; accepted 13 October 2011; published online 21 November 2011)

We carried out direct impurity doping in InAs/GaAs quantum dots (QDs) by selecting the self-assembled growth steps. The photoluminescence (PL) intensity of the Si-doped QDs is enhanced, and thermal quenching of the PL intensity is found to be considerably suppressed, whereas such improvement was not confirmed in Be-doped QDs. The excitation energy dependences of the PL intensity and the time-resolved PL indicate a reduction in the nonradiative recombination probability during the thermalization of carriers generated by high-energy photons. From these results, excess electrons in doped QDs neutralize and, therefore, inactivate the nonradiative recombination centers created by electron traps. © *2011 American Institute of Physics*. [doi:10.1063/1.3660794]

I. INTRODUCTION

Zero-dimensional quantum dots (QDs) are expected to result in high-performance device operation that is stable, highly sensitive, and highly efficient; this is because of the low confinement factor, which in turn is due to the small active volume and the resultant discrete density of states. The doping of impurities into such QDs is necessary for imparting functional properties to the device. In the case of laser and semiconductor optical amplifiers, excess carriers supplied by the dopant compensate for the loss of carriers during device operation.[1,2] This enables high-speed response and modulation of the input signal. In contrast, a highly efficient intersubband transition is useful for ultrafast optical switches and mid-infrared sensors.[3] Recently, intermediate-band solar cells that utilize intersubband optical absorption[4,5] have been attracting considerable attention, as they can enable a highly efficient energy conversion (>60%).[6,7] Furthermore, it is necessary to control the charge in a single QD for single-photon sources and qubits based on electron spin.[8]

The modulation doping technique, which was proposed in 1978,[9] has been successfully implemented for various heterostructure systems; hence, this technique can be used for the manufacture of QD optical devices.[1,2] In the case of using this technique, QD growth is not influenced by doping, because doping is carried out before QD growth. However, it is difficult to control the carrier concentration in each QD, and relatively high doping concentrations of more than 10^{11} cm^{-2} are necessary to obtain obvious effects of doping.[10] On the other hand, if impurities can be doped directly into QDs, the low carrier concentration can be ensured. However, it has been reported that crystal defects caused by direct doping degrades both the crystal quality and the optical properties of QDs.[11,12] Recently, we carried out direct doping of Si into InAs QDs grown by molecular beam epitaxy (MBE), wherein we carefully chose the steps of assembling growth in order to achieve precise direct impurity doping.[13] This self-assembled QD growth process consists of four steps: the nucleation step, assembling step, size-limiting step, and dissolving step.[14] We found that the assembling step is a key step for ensuring efficient impurity doping into QDs. By this direct impurity doping, the emission properties of QDs were improved dramatically and thermal quenching was found to be suppressed.[13] To interpret the improvement, we guessed a possibility of inactivation of defect states by excess carriers. However, the mechanism is still unclear. In this work, we compared effects of doping type on the photoluminescence properties using Si and Be as *n*- and *p*-type dopants, respectively, and the mechanism responsible for enhancement of the emission properties is discussed based on the results of the excitation energy dependences of the PL intensity and the time-resolved PL.

II. GROWTH AND CHARACTERIZATION METHODS

InAs QDs were grown on undoped GaAs (001) substrates by MBE. Before QD growth, an undoped 250-nm GaAs buffer layer was deposited on the substrate at 550 °C. InAs QDs were grown at a substrate temperature of 450 °C and As pressure of 3.0×10^{-6} Torr. The nominal deposition rate was 0.012 monolayers per second (ML/s). In total, 2.4 MLs of InAs were deposited. Here, Si and Be were used as dopants. These dopants are *n*-type and *p*-type, respectively. The impurities were supplied for 15 s in the assembling step. The sheet densities of the doped Si and Be impurities, as measured by secondary ion mass spectroscopy (SIMS), were 4×10^{10} and 2×10^{10} cm^{-2}, respectively, which are almost the same as the QD density shown later.

We confirmed the formation of QDs and the evolution of their shapes by monitoring their reflection high-energy electron diffraction (RHEED) patterns. The surface morphology of uncapped QDs was characterized by scanning probe microscopy measurements in air. Samples used in photoluminescence (PL) measurements were grown on an undoped GaAs (001) substrate under the same growth conditions. The doped QDs were capped by a 150-nm GaAs layer. PL

[a]Author to whom correspondence should be addressed. Electronic mail: kita@eedept.kobe-u.ac.jp.

measurements were performed using a laser diode with emission at 659 nm for excitation. Time-resolved PL measurements were carried out at 3 K using a near infrared streak-camera system with the temporal resolution of 20 ps. The light source used was a mode-locked Ti:sapphire pulse laser with a pulse width of approximately 200 fs and a repetition rate of 80 MHz. An optical parametric oscillator and the frequency doubler were used to create the excitation light pulse with photon energy more than ~1.8 eV.

III. RESULTS AND DISCUSSION

A. Fundamental PL properties of Si-doped QDs and Be-doped QDs

Figure 1 shows tapping-mode atomic force microscopy (AFM) images of (a) undoped QDs, (b) Si-doped QDs, and (c) Be-doped QDs. The QD density was almost independent of the doping condition. We confirmed clear rectification curves in the I-V characteristics at the position of each QD using conductive AFM,[13] when QDs were grown on a doped substrate. As discussed in our previous paper,[13] the current image obtained for the doped QDs was bright, whereas that of the undoped QDs was dark. This indicates that each QD includes excess carriers.

Typical PL spectra of undoped and doped QDs observed at 20 and 280 K are shown in Fig. 2. The PL peak of the Si-doped QDs shows a redshift, and the spectral linewidth becomes narrow with doping. These changes, as observed in the PL spectra, can be explained by the size distribution of the Si-doped QDs.[13] In contrast to the Si-doped QDs, the size-distribution of Be-doped QDs was almost the same as that of the undoped QDs, which was consistent with the PL results. The 20-K PL intensity of the Si-doped QDs was found to become approximately thrice that of the undoped QDs. Since the QD density was almost independent of the doping, the interband radiative recombination process itself is considered to be improved by the Si doping. At low temperature, the non-radiative component of recombination plays a minor role and the PL intensities of undoped and doped samples should become comparable. Therefore, the enhanced PL intensity at the low temperature indicates that deep midgap states[15] created by crystal defects are considered to be inactivated by trapping excess electrons. The emission properties of the Si-doped QDs improved remarkably with the increase in temperature. Figure 3 shows the temperature dependence of the

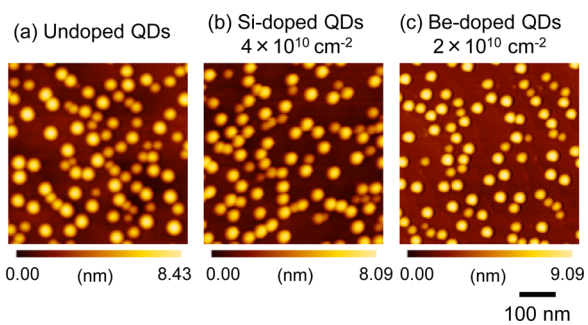

FIG. 1. (Color online) Tapping-mode AFM images of (a) undoped QDs, (b) Si-doped QDs, and (c) Be-doped QDs.

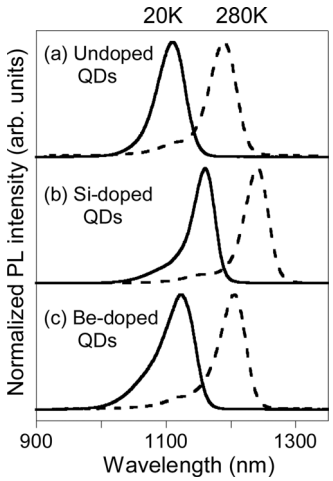

FIG. 2. PL spectra measured at 20 K (solid curves) and 280 K (dashed curves) of (a) undoped QDs, (b) Si-doped QDs, and (c) Be-doped QDs.

PL intensity of undoped QDs, Si-doped QDs, and Be-doped QDs. With increasing temperature, the PL intensity of these QDs decreased, because hot carriers could escape from QDs and were captured into nonradiative centers in the wetting layer or barrier. However, the thermal quenching of the PL intensity of the Si-doped QDs is found to be considerably suppressed. On the other hand, no such improvement in the emission intensity was observed in the case of Be-doped QDs. The thermal activation energy estimated from the temperature dependence of the PL intensity depends on doping.

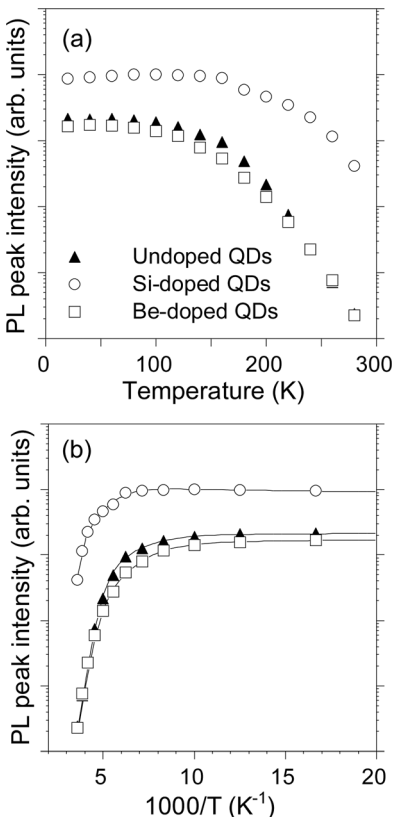

FIG. 3. (a) Temperature dependence of the PL peak intensity of undoped QDs (filled triangles), Si-doped QDs (open circles), and Be-doped QDs (open squares). (b) Arrhenius plots of the PL-peak intensities.

TABLE I. Thermal activation energies estimated from the temperature dependence of the PL intensity.

	Thermal activation energies (meV)	
	ΔE_1	ΔE_2
Undoped QDs	338	73
Si-doped QDs	486	97
Be-doped QDs	327	79

The determined thermal activation energies estimated from the Arrhenius plots of the PL-peak intensities are listed in Table I. ΔE_1 (ΔE_2) can be attributed to thermal activation processes of excitons from the ground state to the GaAs edge (to the excited states). ΔE_1 of the Si-doped QDs is larger than that of the undoped QDs. The improvement in the potential confinement estimated from the PL-peak shift in Fig. 2 was approximately 60 meV, though the energy difference in the activation energy was ~150 meV. Therefore, the relatively small ΔE_1 observed in the undoped QDs indicates the presence of a nonradiative pass in the confinement potential. On the other hand, the thermal activation energies observed for the Be-doped QDs were almost the same as those of the undoped QDs. These results suggest that the nonradiative center is attributed to electron traps.

B. Effects of excess carriers in QDs on PL efficiency

The thermal quenching behaviors in the PL intensity of both the undoped and Si-doped QDs were observed to be suppressed with the increase in excitation density, which are summarized in Figs. 4(a) and 4(b). As shown in Fig. 4(c), the PL intensity of the undoped QDs at 280 K shows a super linear dependence on excitation power, whereas the dependence at the low temperature, 15 K, is linear. However, the dependence of the Si-doped QDs on excitation power was found to have an almost linear trend, even at 280 K (see Fig. 4(d)). These results are similar to the excitation power dependence reported for modulation-doped QDs,[10] where the change in the excitation power dependence was explained by different capture and escape processes. The thermal quenching of PL intensity was suppressed with the increase in the excitation density, because the nonradiative centers were filled with excess carriers. It is clear that the PL temperature quenching of the Si-doped QDs was dramatically suppressed as compared to that of the undoped QDs. The temperature dependence of the undoped QDs obtained under high excitation conditions is similar to the temperature dependences of the doped QDs under low excitation conditions. This suppression of thermal quenching of the PL intensity can be explained by the compensation of carriers lost by both nonradiative and thermal activation processes.

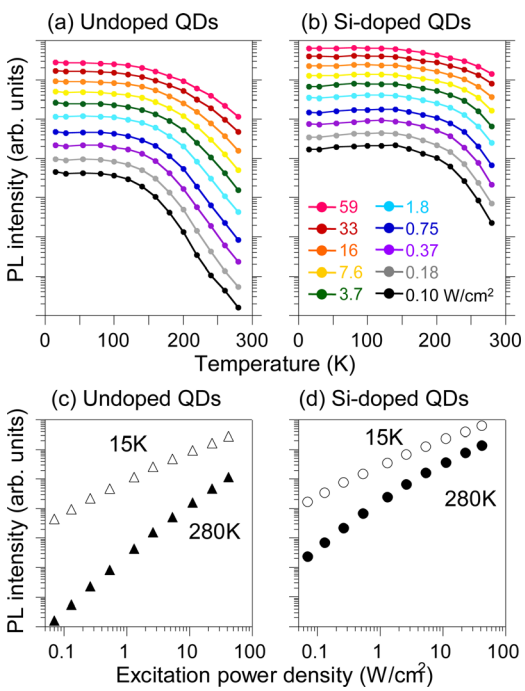

FIG. 4. (Color online) Temperature dependence of PL intensities measured with various excitation densities for (a) undoped QDs and (b) Si-doped QDs. Excitation density dependence of PL intensities measured at 15 K and 280 K for (c) undoped QDs and (d) Si-doped QDs.

C. Compensation of nonradiative electron traps in Si-doped QDs

Next, we compared PL-excitation spectra of undoped QDs and Si-doped QDs. The comparison results are shown in Fig. 5. The results confirmed the occurrence of a remarkable optical absorption at the GaAs-band edge. We found that Si-doping caused a dramatic increase in the PL intensity of QDs excited at high energies. This indicates the reduction in the nonradiative recombination probability during the thermalization of carriers generated by high-energy photons. The penetration depth of excited light decreases with increasing photon energy, and, subsequently, the fraction of excitation light in QDs decreases, owing to the low thickness of the capping layer—150 nm—which roughly corresponds to the penetration depth in GaAs at ~2.2 eV. In other words, nonradiative recombination centers located near the QDs give rise to the reduction in the PL intensity pumped at high excitation energies.

Next, we directly demonstrated the contribution of the nonradiative recombination process using time-resolved PL

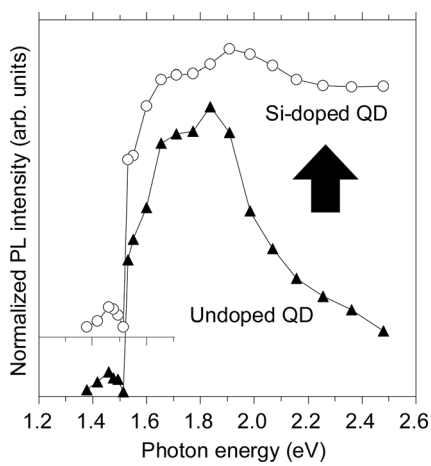

FIG. 5. PLE spectra measured for undoped QDs (filled triangles) and Si-doped QDs (open circles).

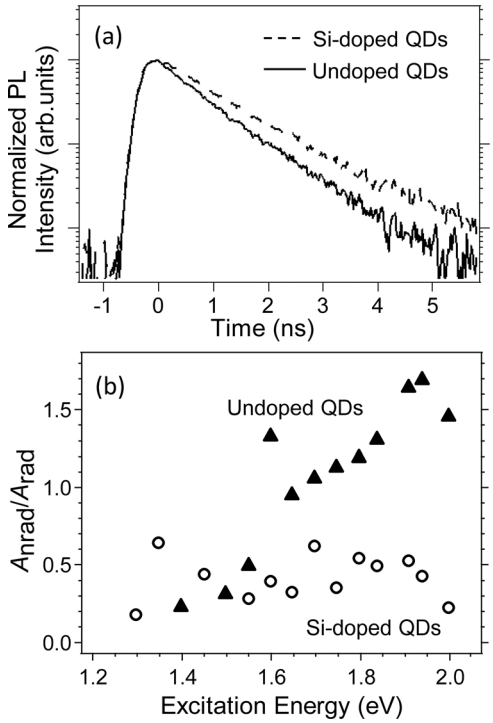

FIG. 6. (a) Typical time-resolved PL profile when excited at 1.8 eV. (b) Ratio of amplitude of nonradiative recombination component to radiative one as a function of the excitation energy.

measurements. Figure 6(a) shows typical time-resolved PL profiles for undoped QDs and Si-doped QDs when excited at 1.8 eV. Here, we kept the excitation photon flux constant. The decay profile was analyzed by fitting with a double exponential function $I(t) = A_{nrad}\exp(-t/\tau_{nrad}) + A_{rad}\exp(-t/\tau_{rad})$, where $A_{rad}(A_{nrad})$ is the number of excitons which recombine with the radiative (nonradiative) process and $\tau_{rad}(\tau_{nrad})$ is the lifetime of the radiative (nonradiative) recombination. Figure 6(b) shows the ratio of the number A_{nrad} to A_{nrad} as a function of the excitation energy. When we evaluate A_{nrad} and A_{rad}, the lifetimes were assumed to be independent of the excitation energy. The estimated τ_{rad} and τ_{nrad} are 1.20(1.00) and 0.65(0.50)ns in Si-doped (undoped) QDs, respectively. The obtained ratios of Si-doped QDs are small as compared with those of undoped QDs. In particular, the difference becomes large with increasing the excitation energy. The small ratio means that the nonradiative recombination process in the high energy was successfully suppressed by the Si doping. These results indicate that excess electrons in doped QDs neutralize and, therefore, inactivate the nonradiative recombination centers created by electron traps.

It is noteworthy that none of the observed dramatic improvements in the emission properties were confirmed in the Be-doped QDs. Similar improvement has been reported for modulation-doped QDs.[10] In the case of such doping, *p*-type doped QDs show advantageous PL characteristics similar to those of *n*-type QDs. The modulation doping method is different from ours, and the doping density of the QDs in the former is about one order of magnitude larger than that in our doping method. Actually, QDs with a high Be concentration of 2×10^{10} cm^{-2} fabricated by the direct doping technique exhibited slight improvement in the temperature dependence of the PL intensity in the present study. Thus, electron doping is very effective to cause the advantageous characteristics. A sort of electron trap is considered to be deactivated by the excess negative charges in *n*-type QDs. This leads to a considerable increase in the PL intensity of the *n*-type QDs, which is consistent with previously reported results for modulation-doped QDs. An enhanced Coulomb attraction[10] due to excess carriers in QDs would become dominant with increasing doping density and/or excitation density.

IV. SUMMARY

We carried out impurity doping into self-assembled InAs/GaAs quantum dots (QDs). Using Si and Be as *n*- and *p*-type dopants, respectively, we compared effects of doping type on the photoluminescence properties. The improved PL emission properties of the Si-doped *n*-type QDs is caused by the filling of nonradiative electron traps with electrons. The excitation energy dependences of the PL intensity and the time-resolved PL demonstrated a reduction in the nonradiative recombination probability during the thermalization of carriers generated by high-energy photons. Thus, we believe that high-performance QD devices can be realized by the direct doping technique, even if each QD includes only a few impurities.

ACKNOWLEDGMENTS

This work was partially supported by the Scientific Research Grant-in-Aid from the Ministry of Education, Culture, Sports, Science and Technology (MEXT) (Grant No. 21360151) and the Incorporated Administrative Agency New Energy and Industrial Technology Development Organization (NEDO), Japan. The authors would like to thank Prof. Kojima for his fruitful discussion.

[1]O. B. Shchekin and D. G. Deppe, Appl. Phys. Lett. **80**, 2758 (2002).
[2]O. B. Shchekin and D. G. Deppe, Appl. Phys. Lett. **80**, 3277 (2002).
[3]O. Wada, A. Suzuki, Y. Ogawa, and K. Tajima, in *Femtosecond Technology*, Springer Series in Photonics, edited by T. Kamiya, F. Saito, O. Wada, and H. Yajima (Springer, Berlin, 1999), p. 59.
[4]S. Maimon, E. Finkman, G. Bahir, S. E. Schacham, J. M. Garcia, and P. M. Petroff, Appl. Phys. Lett. **73**, 2003 (2002).
[5]J. Phillips, J. Appl. Phys. **91**, 4590 (2002).
[6]A. Martí, E. Antolín, C. R. Stanley, C. D. Farmer, N. López, P. Díaz, E. Cánovas, P. G. Linares, and A. Luque, Phys. Rev. Lett. **92**, 186601 (2004).
[7]A. Martí, E. Antolín, C. R. Stanley, C. D. Farmer, N. López, P. Díaz, E. Cánovas, P. G. Linares, and A. Luque, Phys. Rev. Lett. **97**, 247701 (2006).
[8]D. Press, T. D. Ladd, B. Zhang, and Y. Yamamoto, Nature **456**, 218 (2008).
[9]R. Dingle, H. L. Störmer, A. C. Gossard, and W. Wiegmann, Appl. Phys. Lett. **33**, 665 (1978).
[10]Y. D. Jang, J. Park, D. Lee, D. J. Mowbray, M. S. Skolnick, H. Y. Liu, M. Hopkinson, and R. A. Hogg, Appl. Phys. Lett. **95**, 171902 (2009).
[11]J. Phillips, K. Kamath, X. Zhou, N. Chervela, and P. Bhattacharya, Appl. Phys. Lett. **71**, 2079 (1997).
[12]J. S. Kim, P. W. Yu, J.-Y. Leem, J. I. Lee, S. K. Noh, J. S. Kim, G. H. Kim, S.-K. Kang, S. I. Ban, S. G. Kim, Y. D. Jang, U. H. Lee, J. S. Yim, and D. Lee, J. Cryst. Growth **234**, 105 (2002).
[13]T. Inoue, S. Kido, K. Sasayama, T. Kita, and O. Wada, J. Appl. Phys. **108**, 063524 (2010).
[14]T. Kudo, T. Inoue, T. Kita, and O. Wada, J. Appl. Phys. **104**, 074305 (2008).
[15]See http://www.springermaterials.com/navigation/index.html for information about group IV elements, IV-IV and III-V compounds, the Landolt-Börnstein database.